# Towards a NMR-Based Method for Characterizing the Degradation of Nafion XL Membranes for PEMFC

Mylène Robert, Assma El Kaddouri, Jean-Christophe Perrin, Sébastien Leclerc, Olivier Lottin

# Towards a NMR-Based Method for Characterizing The Degradation of Nafion® XL Membranes for PEMFC.

Mylène Robert,[1,2,*] Assma El Kaddouri,[1,2,z] Jean-Christophe Perrin,[1,2] Sébastien Leclerc,[1,2] and Olivier Lottin[1,2,**]

[1]Université de Lorraine, LEMTA, UMR 7563, Vandœuvre-lès-Nancy F-54505, France

[2]CNRS, LEMTA, UMR 7563, Vandœuvre-lès-Nancy F-54505, France

*Electrochemical Society Student Member.

**Electrochemical Society Member.

[z]E-mail: assma.el-kaddouri@univ-lorraine.fr

## Abstract

PFSA-based reinforced membranes are used today as the benchmark material for the electrolyte in PEMFCs. Although greatly improved relatively to their unreinforced version, they still suffer from aging and degradation during fuel cell (FC) operation. In this study we first performed proton NMR to characterize the different water populations in the pristine Nafion XL reinforced membrane. Then we used proton and fluorine NMR, FTIR and sorption measurements in order to qualitatively observe the differences induced in the membrane's chemical structure and properties by long term FC operation. Proton NMR is seen to be an adapted tool to quickly measure a signature that is correlated to the degradation state while FTIR can serve as a local probe of the chemical structure.

*This paper is part of the JES Focus Issue on Proton Exchange Membrane Fuel Cell (PEMFC) Durability.*

## Introduction

The degradation of the proton exchange membrane (PEM) is one of the main factors limiting the proton exchange membrane fuel cell (PEMFC) stability and performance (1, 2). The development of PEM with increased durability remains thus today a critical obstacle that restricts the large scale spreading of PEMFC systems.

The decomposition of the membrane is induced by several factors among which mechanical stress and chemical degradation prevail.

The mechanical degradation is initiated by humidity cycling that creates alternating shrinkage/swelling events and a non-uniform stress distribution in the membrane plane. The resulting reduction of the polymer mechanical strength can lead to the formation of cracks and to the final failure of the membrane electrode assembly (MEA) (3-5).

The chemical decomposition of the PEM in the MEA is caused by gas crossovers. The electrochemical reactions of these gases cause the formation of free radicals and the attack of the polymer chemical structure, which results in scissions in the main chain and in the side chain and finally to the thinning of the membrane (6, 7).

Many studies have focused on PEM chemical degradation and a comprehensive review of the current understanding of the mechanisms in perfluorosulfonic acid (PFSA) membranes was recently published (8). PFSA membranes, such as Nafion, Flemion or Aciplex are today the most widely used fuel cell electrolytes thanks to their good chemical robustness and their high proton conductivity (9). Through the years, efforts have been made to reduce the membrane's ionic resistivity without compromising the mechanical properties. This was made possible by the introduction of chemical stabilizers and mechanical reinforcement. For instance, the Nafion XL is a reinforced membrane composed of two external PFSA layers with stabilizers to reduce chemical attack and a central microporous polytetrafluoroethylene (PTFE)-rich support layer to provide additional mechanical strength and enable the use of thinner ionomer. The central PTFE layer is impregnated with ionomer to provide a continuous conductive pathway across the membrane's thickness.

The structure and basic properties of the Nafion XL membrane were investigated by Shi and co-workers (10). The authors examined the effect of reinforcement and pre-treatment and showed that the reinforcement layer alters significantly the dimensional swelling in the plane while it increases swelling in the thickness direction in such a way that the overall water uptake remains similar to that of the non-reinforced analogue membrane. This swelling anisotropy was shown to be important in reducing the swelling-induced fatigue under cycling fuel cell operation. The same conclusions were drawn in the Gore Select reinforced membrane (11). The analysis of the transport properties reveals that the

58 evolution of the through-plane proton conductivity with the relative humidity is similar for
59 both the XL and the unreinforced N212. This demonstrates that the ionic conduction is still
60 very efficient despite the introduction of the central non-conductive PTFE layer.

61 Although chemically stabilized and reinforced membranes represent advanced evolutions of
62 the PFSA copolymer, reinforced membranes stay nevertheless the target of chemical radicals
63 during FC operation. De Moor et al. (12) studied the degradation of reinforced PFSA
64 membrane on the anode and cathode sides by macroscopic thickness measurements. They
65 demonstrated that, in real systems operating conditions, PFSA degrades first at the anode
66 near the hydrogen inlet which enables hydrogen crossover and leads to the degradation at
67 the cathode. Highly degraded areas were also studied and the results showed that the
68 external PFSA layers disappeared almost completely.

69 The understanding of the impact of the combined effect of mechanical and chemical
70 stressors on the membranes properties is thus critical to improve their durability in FC
71 operation.

72 In the present study we aim at measuring several indicators of the Nafion XL properties in
73 the pristine state and after long term FC operation. The object of our analysis is the
74 evolution of the chemical structure and the water properties due to membrane degradation.
75 For this purpose, we use several experimental techniques, each of which capable of
76 delivering complementary information. The chemical structure is probed using $^{19}$F-NMR to
77 estimate the global ionic exchange capacity (IEC) and IR spectroscopy in the attenuated total
78 reflectance (ATR) mode to look for chemical heterogeneities at the anode and cathode sides
79 of the aged sample. Information on the different water populations in the composite
80 structure is given by the analysis of the $^{1}$H-NMR spectrum and the global water uptake is
81 measured through the sorption isotherm. Finally, we use pulsed-field gradient (PFG)-NMR to
82 characterize the water mobility and diffusion at the micron scale (13). To this point, our goal
83 is not to study the chemical degradation mechanisms but rather to elaborate an
84 experimental approach able to deliver a set of data indicative of membrane degradation.
85 The collection of structural, sorption and transport data on PEM membranes represents a
86 long and tedious process and necessitates quite a lot of resources (analytical instruments
87 and access to large instruments such as synchrotrons (14, 15)). Since the different data are

inter-correlated, we believe that it is possible to gather a set of experimental quantities in a limited amount of time and to define a marker of the membrane degradation based on these data. This paper presents the first steps towards this new approach.

## Experimental

### *Materials*

#### *Perfluorosulfonated membranes*

Two commercial PFSA membranes, Nafion XL and Nafion NR211, were purchased in the protonated ($H^+$) form from Ion Power Inc.. Both membranes present a similar IEC. Nafion NR211 is a monolayer membrane (nominal thickness 25.4 µm) based on chemically stabilized copolymer of tetrafluoroethylene (TFE) and perfluoro(4-methyl-3,6-diaxoct-7-ene) sulfonyl fluoride (16). Nafion XL is a PFSA based membrane with an additional microporous central PTFE layer. The central reinforcement is impregnated both sides with PFSA. The nominal thicknesses are ~12 µm for the PTFE layer and ~9 µm for each external PFSA layer (10, 17) .

A reinforced membrane which operated in Axane Evopac fuel cell system was also investigated. This system, composed of two stacks of 55 cells, was studied in references (18) and (12). It was operated in the field at a constant current density of 0.26 A/cm² during 12 860 hours with approximately 250 start/stop sequences and at an average stack temperature of 60-65 °C. The system was fed at the cathode side with humidified air (60% RH) at a relative pressure of 100 mbar (stoichiometry of 2.5) and at the anode side in dead-end supply mode with pure dry hydrogen at 350 mbar relative pressure (stoichiometry of 1.1). The fuel cell stack was shut down due to recurrent low-level voltage faults. The polarization curves measured at the beginning-of-live and at the end-of-life showed a loss of performance in both stacks. The global voltage decay rate was ~ 3.5 µV/h/cell and ~ 4.5µV/h/cell for the two stacks. The voltage of the cell chosen for the present study decreased slightly from 0.718 to 0.706 V. Based on visual inspection we chose to perform our measurements on a membrane area located near the $H_2$ inlet and air outlet where the degradation was apparent.

#### *Membrane preparation*

The commercial membrane samples were pretreated according to a protocol based on the one established by Xu et al (19, 20). The samples were first boiled in 3 wt. % hydrogen

peroxide solution during 1h and rinsed with distilled water to eliminate any organic impurities. They were then soaked 30 minutes at room temperature in nitric acid (10 mol.L$^{-1}$), rinsed again with distilled water and boiled in deionized water during 1h. In order to ensure a complete substitution of any ionic sites of the ionomer, the samples were boiled in sulfuric acid (1 mol.L$^{-1}$) during 1h before boiling during 1h in distilled water to clean the sample. Finally, the samples were dried 24 h in an oven at 60°C.

The aged membrane was extracted from the MEA by carefully removing the gas diffusion/electrode layers with a brush soaked in a water/ethanol mixture. It was then rinsed with deionized water, dried at 60°C overnight and rehydrated in deionized water prior to measurement. The sample investigated here (~1 cm x 1 cm) was cut from a specific area near the dry hydrogen inlet and air outlet.

*Water Sorption*

The water sorption isotherms were measured using a IGASorp (Hiden Isochema, UK) dynamic vapor sorption (DVS) analyzer. The samples were first dried several hours under dry nitrogen at a temperature of 24°C. The water isotherms were recorded at 24°C for a water activity range between 0 and 0.95. The water content $\lambda$, characterizing the number of water molecules per sulfonic acid group, is determined from the water uptake $\frac{\Delta m}{m_0}$ using the following relation:

$$\lambda = \frac{n(H_2O)}{n(SO_3^-)} = \frac{\Delta m/18}{IEC * m_0}$$

where $IEC$ is the ion exchange capacity of the considered membrane expressed in eq/g, $\Delta m$ is the mass variation measured in g, $m_0$ is the membrane dry weight in g and the molecular weight of water molecule is 18 g/mol.

*FTIR-ATR*

FTIR-ATR spectra were obtained with a Spectrum One (Perkin Elmer) spectrometer equipped with a DTGS detector and using a single reflection diamond ATR accessory. The spectra were recorded with a wavenumber resolution of 1 cm$^{-1}$ in the spectral range [650 – 4000 cm$^{-1}$]. The measurements were performed at various locations on the surface of the commercial membrane samples to check the homogeneity of the chemical structure. In the

case of the aged sample, the measurements were also performed in various areas of the surface to ensure reproducibility and on both membrane sides to investigate aging heterogeneities.

*NMR Spectroscopy*

*Solid-state $^{19}$F-NMR*

The spectra were measured at 282.37 MHz on a Bruker Avance III 300WB spectrometer equipped with a 2.5 mm X-H/F double-resonance probe. The samples were rolled and packed in a zirconia rotor with Vespel end-caps. All experiments were performed at 24°C using a magic-angle spinning (MAS) rate of 25 kHz. The spectra were recorded using a specific Hahn-echo pulse sequence, which consists in repeating the echo cycle to suppress background signals coming from the probe. The $^{19}$F 90° pulse length was 5 µs and the echo cycle was repeated 5 times during the measurement. 256 scans were recorded and averaged with a recycle delay of 4 s and a dwell time of 3.3 µs.

*Liquid-state $^{1}$H-NMR*

The experiments were carried out on a Bruker Avance III 600WB spectrometer operating at the Larmor frequency of 600.13 MHz and using a 5 mm Diff30 probe able to deliver a maximum gradient intensity of 1800 G/cm. The spectra were recorded at 24°C using 32–64 scans with a recycle delay of 3 s and a dwell time of 25 µs. The proton 90° pulse width was optimized for each sample. Each sample was first fully immersed in distilled water at room temperature during 60 to 90 minutes. The sample size was approximately 1 x 1 cm for both the pristine and aged XL membranes. Once out of the water, the samples were quickly pressed between two layers of absorbent paper to remove residual water droplets from the surface before being rolled and packed into 5 mm airtight tubes.

*PFG-NMR*

The water self-diffusion coefficients were measured using a stimulated-echo sequence (PGSTE) with unipolar gradients and calculated from a plot of the observed signal attenuation as a function of the applied gradient strength g. The experiments were performed with a pulse time $\delta$ = 1.0 – 1.6 ms, a diffusion delay $\Delta$ = 5 – 10 ms and a gradient strength 20 - 700 G/cm. The water self-diffusion coefficient $D_s$ was obtained from a fit of the

experimental data using the Stejskal – Tanner equation (21). The error on diffusion measurements is estimated to be on the order of 5%, the main source of errors being the gradient calibration and the control of both temperature and water content.

*NMR relaxation*

The $^{1}H$ spin-lattice relaxation times ($T_1$) were measured at 24°C using the inversion-recovery pulse sequence. 8 scans were recorded with a recycle delay of 2 or 3 s (depending on the sample) and a dwell time of 25 μs. The relaxation time $T_1$ was determined by fitting the experimental evolution of the signal attenuation as a function of the relaxation delay τ using single or bi-exponential functions, depending on the situation (see Results).

## Results

*Water populations and mobility.*

Figure 1-a presents a set of $^{1}H$-NMR measurements on the water saturated Nafion XL membrane. The static spectrum shows two resonances lines. The chemical shift of the most intense component at 4.69 ppm corresponds approximately to that observed in non-reinforced hydrated PFSA membranes at equivalent temperature and water content: Nafion NR211 (6.20 ppm), Gore 800 (5.83 ppm at 98% RH) (22).

In unreinforced Nafion, water is known to exist in different states (23-26), namely non-freezing water, bound freezing water and free water. Although dielectric relaxation spectroscopy is able to describe different responses relative to these populations, the spectral resolution of proton NMR performed at room temperature is not high enough to detect them directly. Because the exchange time between these populations is fast compared to the NMR time scale (ms) they all appear at about the same chemical shift and the proton spectrum is composed of a single component.

The second resonance observed at 6.40 ppm is much weaker than the main component. The higher chemical shift indicates a deshielding of the water protons and thus less electron density around them. This could come from a denser hydrogen bond network and/or a different local environment for the water in the central layer. Given the complex microstructure of the porous PTFE layer (see for example Fig. 10 of Reference (10)) and the pore size [10 nm - 1 μm] some of the water adsorbed in the reinforcement is presumably in

a confined state with water-ionomer interactions that are different in the central layer than in the two external layers. These interactions would result in stronger hydrogen bonds and lead, on average, to a higher NMR chemical shift.

The ratio of the area of the two lines corresponds in principle to the ratio of the two water populations. In the water-saturated Nafion XL, the measured ratio is approximately 3.4 %. Given the relative thickness of the central layer $l/L$ = 0.33 in the water saturated state (10) and the high porosity of the PTFE matrix, it is likely that only a fraction of the water adsorbed in the central layer contributes to this second peak.

The longitudinal NMR relaxation time $T_1$ is indicative of the proton molecular translational and rotational dynamics at a time scale corresponding to the inverse NMR frequency ($\sim$ 1 ns at a NMR frequency of 600 MHz). Figure 1-b presents the $T_1$ measurements for the two water populations. The longitudinal relaxation is mono-exponential for population 1, with a relatively short relaxation time (18.9 ms). Interestingly, the NMR relaxation of the second water population presents a bi-exponential behavior with one-time constant equivalent to that of population 1 and a second, much longer, indicative of water with a faster dynamic.

This complex behavior proves that two water populations contribute to the low amplitude resonance line of the $^{1}H$ spectrum (populations 2.1 and 2.2). The PFG-NMR diffusion experiments help to clarify the situation. Figure 1-c presents the raw spectra, recorded at different magnetic field gradient values. The data clearly show that the two resonances are attenuated in the course of the experiment, thus proving that populations 1 and 2 correspond to water diffusing at the time scale of the measurement (several ms). The calculated area of the peaks is plotted on Figure 1-d versus the magnetic field gradient and the experimental points are fitted using the Stejskal – Tanner equation. Water from population 1 presents a simple behavior and the single exponential fit gives a diffusion coefficient of 2.32 x $10^{-10}$ m²/s. This value corresponds to what is usually measured in the unreinforced water-saturated Nafion (13, 20, 27-30). As already observed in the relaxation data, the behavior of population 2 is more complex and the fit to the data must be made with two exponential components. Again two water populations are detected. Population 2.1 diffuses with a diffusion coefficient which is about half the value of population 1. This is coherent with the two similar relaxation times, the lower value of the diffusion coefficient

being due to confinement in the porous PTFE. Population 2.2 is diffusing very fast, its diffusion coefficient being approximately one third of the coefficient of bulk water at the same temperature (0.77 x $10^{-9}$ m²/s versus 2.30 x $10^{-9}$ m²/s). The high diffusion coefficient and the long relaxation time are indicative of a water population which is relatively free to move. Thus, it is possible to assign it to a small amount of free water which may exist at the interface between the ionomer and the PTFE reinforcement or present in voids spaces that were not filled with PFSA during the casting of the membrane.

Figure 2 presents $^{1}$H-NMR data measured in the water-saturated reinforced membrane extracted from the aged MEA after 12,860 hours of operation. The proton spectrum shows two resonance lines (Figure 2-a). Population 1 resonates at a lower field than in the pristine membrane ($\delta H$ = 4.07 ppm versus 4.69 ppm) while the chemical shift of population 2 remains approximately the same. Furthermore, the relative area of the two resonances increases significantly after FC operation ($\sim$ 7% of the total water content versus 3.4%). These two observations are consecutive of changes that occurred in the membrane's microstructure during FC operation. They could either indicate a decrease of the quantity of ionomer in the external layers and/or a partial loss of the membrane sorption properties. In Figure 2-b the diffusion data show the corresponding changes in the diffusion properties for the two water populations.

In coherence with the proton spectrum, the diffusion coefficient of population 1 is lower in the aged membrane. Again, this is indicative of less water content and/or changes in the diffusion pathways in the PFSA structure. The water sorption isotherm presented in Figure 3 can help to understand these observations. In the Nafion PFSA, the water sorption behavior is one of the most important phenomenon affecting its structural and transport properties. This complex curve is highly non-linear as a result of complex interactions between the water, the hydrophilic ionic sites and the hydrophobic matrix. It is often described as a three-steps process (9): the ionization of the sulfonic acid groups at very low water activity ($a_w$), the formation of multiple solvation shells in an interconnected water network at intermediate water activity and, finally, the growth and the increase in the connectivity of the hydrophilic domains by adding bulk-like water at high hydration levels. The first step involves strong interactions caused by hydrogen bonds and can be described by the Langmuir adsorption process. The second step corresponds to the dissolution of water in the

polymer phase and can be modelled by the Henry's linear equation (31, 32). The final upturn of the isotherm at higher water activities is linked to the macroscopic swelling of the membrane and thus is controlled by the membrane's mechanical properties (9).

The experimental isotherms of Figure 3 show that the maximum water uptake is much lower in the aged membrane than in the pristine sample. This is mostly due to the partial loss of the Langmuir contribution ($a_w$ < 0.1) and the reduction of the Henry's slope (shown in bold lines for 0.15 < $a_w$ < 0.65), which can be linked to a decrease in the hydrophilic character of the membrane and a loss of ionic groups due to the scission of polymer chains. Interestingly, the final upturn at high $a_w$ was not impacted after operation, which means that even if structural changes are induced by long term operation, they don't seem to alter the polymer matrix's resistance.

*Chemical structure analyses*

*$^{19}$F-NMR spectroscopy*

The chemical structure of the PFSA polymer can be characterized by $^{19}$F-NMR spectroscopy (Figure 4). The chemical shifts of the pristine XL reinforced membrane are assigned and identified in Figure 4 on the basis of Chen and Schmidt-Rohr's investigation (33). This assignment is characteristic of the long side chain (LSC) – PFSA ionomer as well as the PTFE signature outlined by a higher intensity ratio $I_{(CF_2)_n\ at-117ppm}/I_X$ compared to the Nafion NR211 monolayer. PFSA membranes can be characterized through the IEC parameter measured from the $^{19}$F NMR spectra. Indeed, the IEC is related to the number of moles of TFE *n* per mole of comonomer unit by:

$$\mathrm{IEC} = \frac{1000}{100 \times \mathrm{n} + \mathrm{M}}$$

where M corresponds to the molecular weight of vinyl ether monomer (M = 444 g.mol$^{-1}$) and $n$ can be calculated thanks to the resonance peak area $I_{CF_3+OCF_2}$ and $I_{CF_2+(CF_2)_n}$ with a theoretical relationship deduced from the chemical structure of the LSC – PFSA ionomer. This relationship was also previously validated by solid-state $^{19}$F NMR on PFSA membranes (17).

In the case of reinforced membranes, the IEC does not correspond only to the PFSA ionomer since the resonance peak area at -117 ppm inevitably takes into account the NMR signal of the PTFE reinforcement. Without knowing the proportion of PTFE per unit of PFSA, it is not possible to separate the $(CF_2)_n$ PFSA from the PTFE signals. Therefore, the IEC measured in the case of reinforced membranes corresponds to a "global IEC" ($IEC_g$) of the tri-layer membrane (17). Even though NMR does not directly provide the IEC of the LSC – PFSA, the $IEC_g$ allows us to estimate the degree of chemical degradation in a comparative study after FC operation. The experimental measurement of the IEC of NR211 and $IEC_g$ of XL membranes are in agreement with, respectively, the supplier data sheet and literature values (17), as indicated on Figure 4.

After 12,860 hours of FC operation, the spectrum shows a similar structure with the same resonance peaks and chemical shifts (Figure 4) but with lower normalized intensities associated to the – $OCF_2$ / – $CF_3$ (-73 ppm) and $SCF_2$ (-112 ppm) groups. These variations point out a change in the chemical structure related to side chain groups which seems to correspond to a partial loss of side chains. The chemical degradation by side chains loss has already been observed for monolayer PFSA in previous ex-situ and in-situ studies (7, 8, 34-36). The decrease of the $IEC_g$ from 0.87 to 0.83 indicates here that the global IEC is only slightly impacted by FC operation.

*FTIR-ATR spectroscopy*

The FTIR investigation was carried out in order to measure exclusively the chemical degradation of the ionomer part of the reinforced membrane. The ATR mode was used to characterize the PFSA outer layers on both sides of the reinforced membrane and in different areas to ensure reproducibility. The data are plotted in the 4000-650 $cm^{-1}$ frequency range on Figure 5-a. The spectra were normalized to the asymmetric $CF_2$ stretching mode (1145 $cm^{-1}$). As expected, they exhibit the characteristic signal of the LSC – PFSA type ionomer. The assignment is detailed in Table 1 based on literature (37-40). All studies agree on the absorption bands assignment except for the peak located at $\sim$ 980 $cm^{-1}$ whose attribution is still open to discussion. Some authors (39, 41, 42) attributed this peak to the stretching mode of C–O–C group close to the main chain while others assigned it to CF stretching mode of the $CF_2$–$CF(CF_3)$– group (38, 43). The cathode and anode side spectra

measured after FC operation are plotted on Figure 5, and compared to the pristine XL membrane. In Figure 5-b, after FC operation we observe a significant decrease of the S–O and C–O–C stretching bands intensities as well as a small decrease of the absorption band at ~980 $cm^{-1}$. The decrease of these characteristic bands confirms that the chemical degradation corresponds to a partial loss of the side chains. As plotted in the insert Figure 5-a, two new bands were detected on aged samples in the range of 2850 to 3000 $cm^{-1}$ attributed to symmetric and asymmetric CH stretching modes corresponding to C-H vibration band already observed and identified as chemical degradation observed after ageing (34, 44, 45). Furthermore, FTIR data highlights decrease of O-H signal relative to liquid water (4000-2500 $cm^{-1}$) in membrane after fuel cell operation. This confirms the water sorption loss measured by DVS. Figure 5-a and Figure 5-b also show a large similitude in the spectra measured on the anode and cathode sides, showing a similar degradation on both sides on the membrane.

A specific area of the sample, where the PFSA external layers have partially disappear, was also probed. The spectra corresponding to the anode and cathode sides are plotted on Figure 5. A drastic decrease is observed in the characteristic PFSA signals as well as an intensity drop of the S–O stretching / C–O–C stretching / band at ~ 980 $cm^{-1}$ and a sharpening of the $CF_2$ stretching signals (1210 and 1145 $cm^{-1}$). These spectra thus present the characteristic features of PTFE with a small presence of S–O stretching / C–O–C stretching bands. In this degraded area the PFSA layers are thus almost completely lost, in coherence with what is visually observed.

**Discussion**

The multi-techniques characterization shows that the reinforced PFSA membrane undergoes a modification of its chemical structure during FC operation, which significantly impacts its sorption and transport properties.

The fluorine NMR and FTIR spectroscopies provide experimental clues for a chemical degradation of the PFSA ionomer by side chain scission (on ether groups or/and carbon-sulfur bond). This results in a partial loss of the ionic sulfonic groups and a decrease of the maximum water uptake as observed on the sorption isotherm and through the intensity ratio of the two resonance lines in the proton NMR spectrum. In addition, the proton NMR

analysis suggests that the sorption properties of the outer layers (whose water contributes the most to component 1) are predominantly affected since the NMR signature assigned to water in the central layer is not significantly changed after FC operation. The mechanical cohesion of the polymeric matrix, however, is not altered since the final upturn of the sorption isotherm is not modified. This is confirmed by the NMR relaxation and diffusion measurements which show that the adsorbed water does not present a free water behavior as it would be in a porous-like structure with less mechanical cohesion and less water confinement.

*Contribution of the used experimental techniques to the characterization of membrane aging*

- The evolution of the chemical structure in PFSA ionomers is often investigated using $^{19}$F-NMR spectroscopy since the IEC can be quantitatively measured. In the case of reinforced membranes, the IEC determination is made difficult using this method because of the contribution of the PTFE in the central layer. Thus, without the precise knowledge of the relative PTFE content in the central layer and in the outer layers, the signature of the chemical degradation appears only qualitatively on the raw NMR spectrum. Therefore, the FTIR analysis is more relevant even though it is not easily quantitative. Moreover, FTIR is a local probe of the chemical structure, while $^{19}$F-NMR only provides averaged information. It allows the investigation of both sides of the membrane exposed to anode and cathode electrodes. One can thus probe possible differences between both sides and heterogeneities in the plane.
- $^{1}$H-NMR appears to be a fast and efficient technique to investigate the different water populations, in the external layers and in the ionomer dispersed in the PTFE reinforcement. The relative areas and the difference in NMR chemical shift of the two resonance lines can be used as indexes to quickly quantify the water content. As aging is seen to impact the sorption properties of the external layers, these two parameters can be defined as indicators of the aging condition of the membrane.
- Water mobility is related to both the water content and the microstructure of the polymer matrix. The simultaneous determination of the membrane's water content from the proton spectrum and of the water diffusion coefficient from PFG-NMR experiments represents efficient means of quantifying the changes in the structure-transport relationship due to aging.

- The complex nature of the small water signal at lower field in the proton NMR spectrum was revealed by the NMR relaxation and diffusion measurements. We saw that at least two water populations contributed to this peak. To supplement the information obtained from the 1D spectrum, more advanced techniques can be used (46). Relaxation-diffusion 2D spectra for instance can give interesting correlations between the molecular rotational dynamics and the nanosecond time scale and the long-range diffusion (millisecond time scale and micrometer length scale). Such experiments will be performed in a near future to elucidate with more details the nature of this peak. Exchange experiments should also provide information about the exchange time between the different water reservoirs.
- In the present experiments, the presence of a small quantity of highly mobile water in the central reinforcement or at the interface reinforcement/external layers is detected in both the pristine and aged membranes. Our ability to detect free water, either in the external layers or at the interface with the mechanical reinforcement can be very useful in order to characterize the membrane's degradation. When the microstructure is modified due to the scission of polymer chains, the confinement of the water molecules is less pronounced as the matrix's resistance to swelling is lowered: this could effectively result in more bulk-like water and a higher mobility. The detection of more free water in the membrane's structure can thus become an indicator of its mechanical degradation.

**Conclusion**

We performed an experimental study of some of the important properties of PFSA reinforced membranes before and after long-term operation (12,860 hours) in a fuel cell. Our objective was to demonstrate that a small quantity of fast measurements can bring relevant information on the impact of FC operation on these properties. To our knowledge this is the first time that proton NMR is used to study the different water states and their dynamics in the Nafion XL membrane.

From our measurements we conclude that:

- The PFSA reinforced membrane, although chemically and mechanically reinforced, endures chemical degradations leading to a decrease of its sorption capacity. This is due to the partial loss of the ionic sulfonic groups caused by side-chain scissions. The mechanical

integrity of the membrane is not severely impacted and the adsorbed water does not lose its confinement.

- Proton NMR is powerful to detect the different water states in this membrane as the water present in the central reinforcement gives a NMR signature distinct from the one present in the outer layers. The relative area of the two resonances gives indications on the water fraction in the two locations. In aged reinforced membranes, this measurement can thus serve as a marker to quantify the degree of degradation.
- The relaxation and diffusion data give insights on the water dynamics at the nanoseconds and microseconds, respectively. We observe that water in the external layers of the pristine Nafion XL behaves as in the unreinforced Nafion. The second signal is more complex and two distinct populations exist with very different dynamics. A small proportion of it is highly mobile while the rest presents a signature similar to that of the water in the external layers. In the aged sample, the majority of the water (component 1) is less mobile because of lower water content. More detailed measurements are needed at this stage to elucidate the exact nature of these components. More specifically it will be relevant to perform correlation experiments in order to study the exchange between the different water reservoirs.

Based on our findings, we think that it is possible to use proton NMR and FTIR to quickly characterize the degradation state of PFSA reinforced membranes. More experiments are being performed in our institution in order to study the evolution of the NMR parameters as a function of the hydration in the pristine membrane. The set of data will be use as a calibration of the reference properties.

**Acknowledgements**

The authors would like to thank the LEPMI/LMOPS (http://www.lmops.univ-savoie.fr) and the CRM2/NMR methodology groups (http://crm2.univ-lorraine.fr/lab/fr/research/rmn/), the H2E project for providing the membrane samples after FC operation and Axane fuel cell systems.

**References**

1. R. Borup, J. Meyers, B. Pivovar, Y. S. Kim, R. Mukundan, N. Garland, D. Myers, M. Wilson, F. Garzon, D. Wood, P. Zelenay, K. More, K. Stroh, T. Zawodzinski, J. Boncella, J. E. McGrath, M. Inaba, K.

441 Miyatake, M. Hori, K. Ota, Z. Ogumi, S. Miyata, A. Nishikata, Z. Siroma, Y. Uchimoto, K. Yasuda, K. I.
442 Kimijima and N. Iwashita, *Chemical Reviews*, **107**, 3904 (2007).
443 2. L. Dubau, L. Castanheira, F. Maillard, M. Chatenet, O. Lottin, G. Maranzana, J. Dillet, A.
444 Lamibrac, J. C. Perrin, E. Moukheiber, A. ElKaddouri, G. De Moor, C. Bas, L. Flandin and N. Caque,
445 *Wiley Interdisciplinary Reviews-Energy and Environment*, **3**, 540 (2014).
446 3. A. Kusoglu, M. Calabrese and A. Z. Weber, *Ecs Electrochemistry Letters*, **3**, F33 (2014).
447 4. E. Moukheiber, C. Bas and L. Flandin, *International Journal of Hydrogen Energy*, **39**, 2717
448 (2014).
449 5. M. V. Williams, H. R. Kunz and J. M. Fenton, *Journal of Power Sources*, **135**, 122 (2004).
450 6. L. Ghassemzadeh, T. J. Peckham, T. Weissbach, X. Y. Luo and S. Holdcroft, *Journal of the*
451 *American Chemical Society*, **135**, 15923 (2013).
452 7. L. Ghassemzadeh, K. D. Kreuer, J. Maier and K. Muller, *Journal of Physical Chemistry C*, **114**,
453 14635 (2010).
454 8. M. Zaton, J. Roziere and D. J. Jones, *Sustainable Energy & Fuels*, **1**, 409 (2017).
455 9. A. Kusoglu and A. Z. Weber, *Chemical Reviews*, **117**, 987 (2017).
456 10. S. W. Shi, A. Z. Weber and A. Kusoglu, *Journal of Membrane Science*, **516**, 123 (2016).
457 11. Y. L. Tang, A. Kusoglu, A. M. Karlsson, M. H. Santare, S. Cleghorn and W. B. Johnson, *Journal*
458 *of Power Sources*, **175**, 817 (2008).
459 12. G. De Moor, C. Bas, N. Charvin, J. Dillet, G. Maranzana, O. Lottin, N. Caque, E. Rossinot and L.
460 Flandin, *International Journal of Hydrogen Energy*, **41**, 483 (2016).
461 13. M. Klein, J. C. Perrin, S. Leclerc, L. Guendouz, J. Dillet and O. Lottin, *Macromolecules*, **46**, 9259
462 (2013).
463 14. G. S. Hwang, D. Y. Parkinson, A. Kusoglu, A. A. MacDowell and A. Z. Weber, *Abstracts of*
464 *Papers of the American Chemical Society*, **245** (2013).
465 15. S. Lyonnard and G. Gebel, *European Physical Journal-Special Topics*, **213**, 195 (2012).
466 16. Du Pont, Product Information: Nafion NR-211 and NR-212, PFSA Membrane, in (2010).
467 17. E. Moukheiber, G. De Moor, L. Flandin and C. Bas, *Journal of Membrane Science*, **389**, 294
468 (2012).
469 18. L. Dubau, L. Castanheira, M. Chatenet, F. Maillard, J. Dillet, G. Maranzana, S. Abbou, O. Lottin,
470 G. De Moor, A. El Kaddouri, C. Bas, L. Flandin, E. Rossinot and N. Caque, *International Journal of*
471 *Hydrogen Energy*, **39**, 21902 (2014).
472 19. F. Xu, C. Innocent, B. Bonnet, D. J. Jones and J. Roziere, *Fuel Cells*, **5**, 398 (2005).
473 20. F. N. Xu, S. Leclerc, O. Lottin and D. Canet, *Journal of Membrane Science*, **371**, 148 (2011).
474 21. E. O. Stejskal and J. E. Tanner, *Journal of Chemical Physics*, **42**, 288 (1965).
475 22. Z. R. Ma, R. C. Jiang, M. E. Myers, E. L. Thompson and C. S. Gittleman, *Journal of Materials*
476 *Chemistry*, **21**, 9302 (2011).
477 23. Z. Lu, G. Polizos, E. Manias and D. D. Macdonald, *Batteries and Energy Technology (General) -*
478 *217th Ecs Meeting*, **28**, 81 (2010).
479 24. Z. J. Lu, G. Polizos, D. D. Macdonald and E. Manias, *Journal of the Electrochemical Society*,
480 **155**, B163 (2008).
481 25. M. Laporta, M. Pegoraro and L. Zanderighi, *Physical Chemistry Chemical Physics*, **1**, 4619
482 (1999).
483 26. Y. S. Kim, L. M. Dong, M. A. Hickner, T. E. Glass, V. Webb and J. E. McGrath, *Macromolecules*,
484 **36**, 6281 (2003).
485 27. L. Maldonado, J. C. Perrin, J. Dillet and O. Lottin, *Journal of Membrane Science*, **389**, 43
486 (2012).
487 28. Q. A. Zhao, P. Majsztrik and J. Benziger, *Journal of Physical Chemistry B*, **115**, 2717 (2011).
488 29. T. A. Zawodzinski, M. Neeman, L. O. Sillerud and S. Gottesfeld, *Journal of Physical Chemistry*,
489 **95**, 6040 (1991).
490 30. J. E. Hensley, J. D. Way, S. F. Dec and K. D. Abney, *Journal of Membrane Science*, **298**, 190
491 (2007).

31. M. Legras, Y. Hirata, Q. T. Nguyen, D. Langevin and M. Metayer, *Desalination*, **147**, 351 (2002).
32. D. R. Morris and X. D. Sun, *Journal of Applied Polymer Science*, **50**, 1445 (1993).
33. Q. Chen and K. Schmidt-Rohr, *Macromolecules*, **37**, 5995 (2004).
34. M. Danilczuk, L. Lancuki, S. Schlick, S. J. Hamrock and G. M. Haugen, *Acs Macro Letters*, **1**, 280 (2012).
35. T. Xie and C. A. Hayden, *Polymer*, **48**, 5497 (2007).
36. J. Healy, C. Hayden, T. Xie, K. Olson, R. Waldo, A. Brundage, H. Gasteiger and J. Abbott, *Fuel Cells*, **5**, 302 (2005).
37. K. A. Mauritz and R. B. Moore, *Chemical Reviews*, **104**, 4535 (2004).
38. Z. X. Liang, W. M. Chen, J. G. Liu, S. L. Wang, Z. H. Zhou, W. Z. Li, G. Q. Sun and Q. Xin, *Journal of Membrane Science*, **233**, 39 (2004).
39. K. M. Cable, K. A. Mauritz and R. B. Moore, *Journal of Polymer Science Part B-Polymer Physics*, **33**, 1065 (1995).
40. M. Ludvigsson, J. Lindgren and J. Tegenfeldt, *Electrochimica Acta*, **45**, 2267 (2000).
41. C. Chen and T. F. Fuller, *Polymer Degradation and Stability*, **94**, 1436 (2009).
42. N. Ramaswamy, N. Hakim and S. Mukerjee, *Electrochimica Acta*, **53**, 3279 (2008).
43. L. Y. Levy, A. Jenard and H. D. Hurwitz, *Journal of the Chemical Society-Faraday Transactions I*, **78**, 29 (1982).
44. L. Ghassemzadeh, K. D. Kreuer, J. Maier and K. Muller, *Journal of Power Sources*, **196**, 2490 (2011).
45. F. M. Collette, C. Lorentz, G. Gebel and F. Thominette, *Journal of Membrane Science*, **330**, 21 (2009).
46. R. Fechete, D. E. Demco, X. M. Zhu, W. Tillmann and M. Moller, *Chemical Physics Letters*, **597**, 6 (2014).

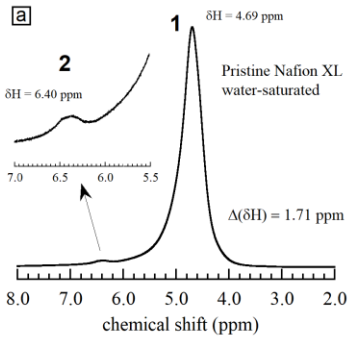


518

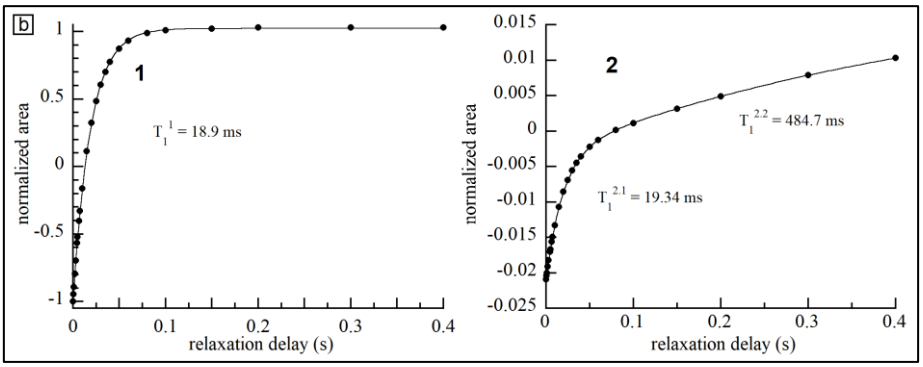


519

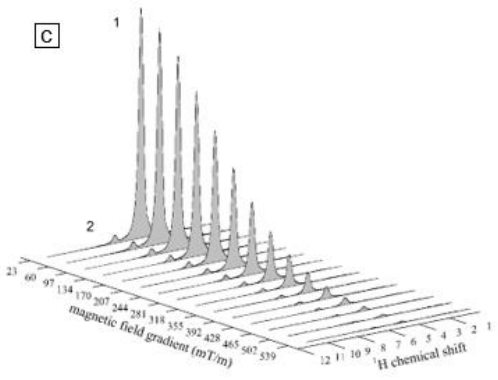


520

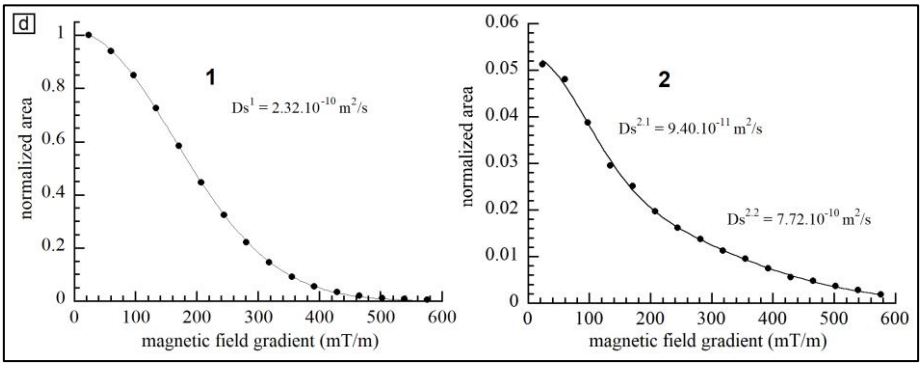


521

522 *Figure 1.* ***$^1$H-NMR experiments in the water-saturated Nafion XL reinforced membrane (600 MHz).***
523 ***a- Static $^1$H-NMR spectrum. b- $T_1$ relaxation experiments. c- Raw water diffusion data. d- Fitted***
524 ***diffusion data.***

525

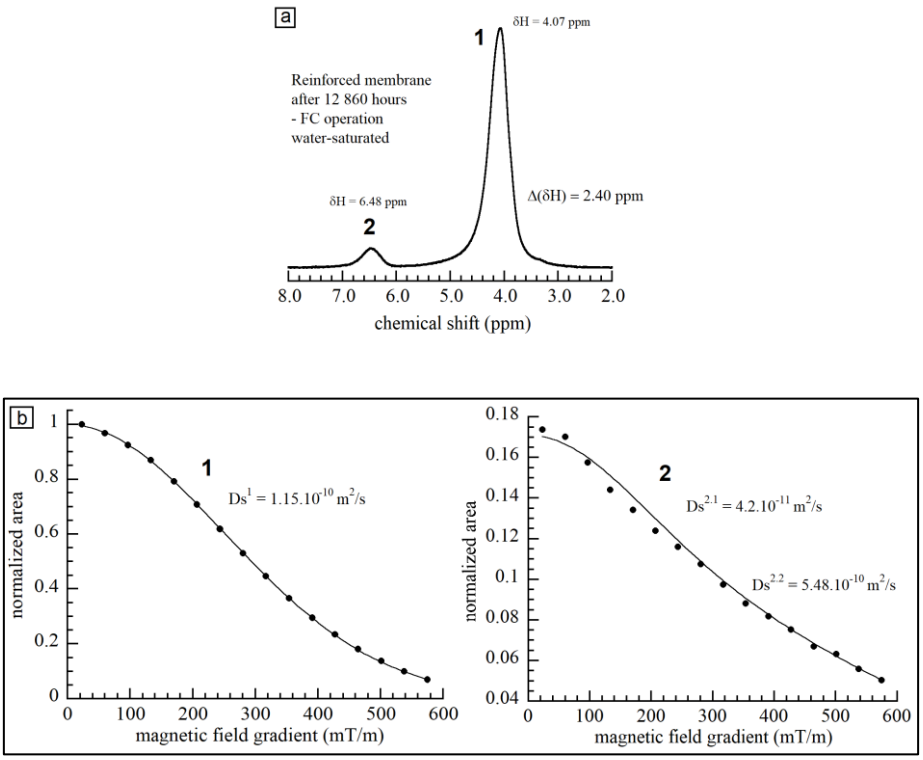


*Figure 2.* ***$^{1}$H-NMR experiments in the water-saturated reinforced membrane after long-term FC operation. a- Static $^{1}$H-NMR spectrum. b- Diffusion data.***

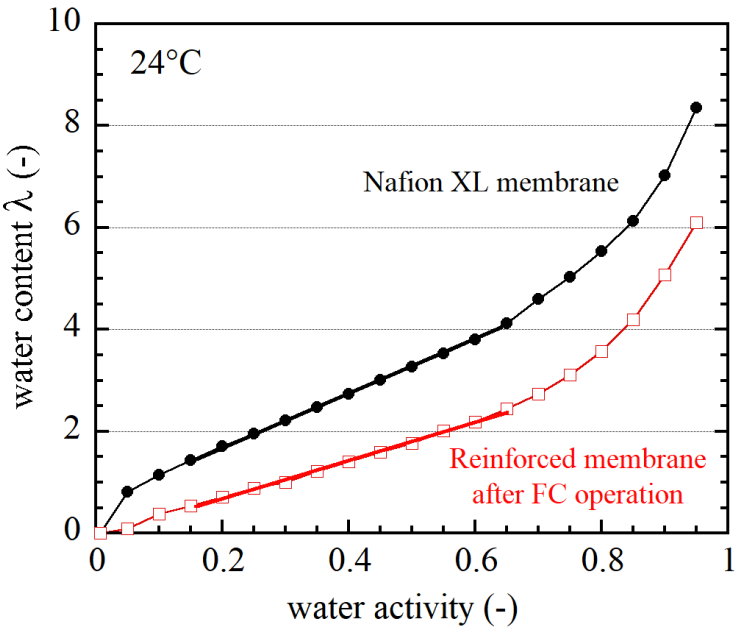


*Figure 3*. ***Water sorption isotherms at 24°C of Nafion XL reinforced membrane and reinforced membrane after long-term FC operation.***

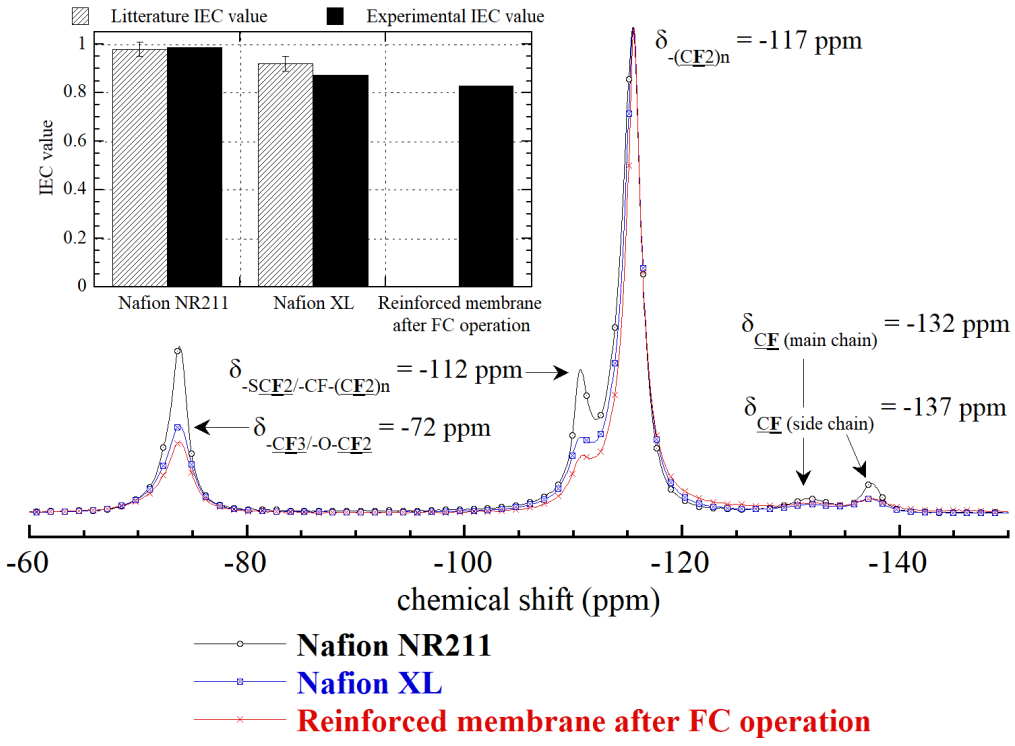


*Figure 4.* ***$^{19}$F-NMR spectra of Nafion NR211, Nafion XL reinforced membrane and reinforced membrane after FC operation. The bars compare the measured IEC of NR211 and XL membranes to the literature values (10, 16, 17) and the IEC of reinforced membrane after FC operation.***

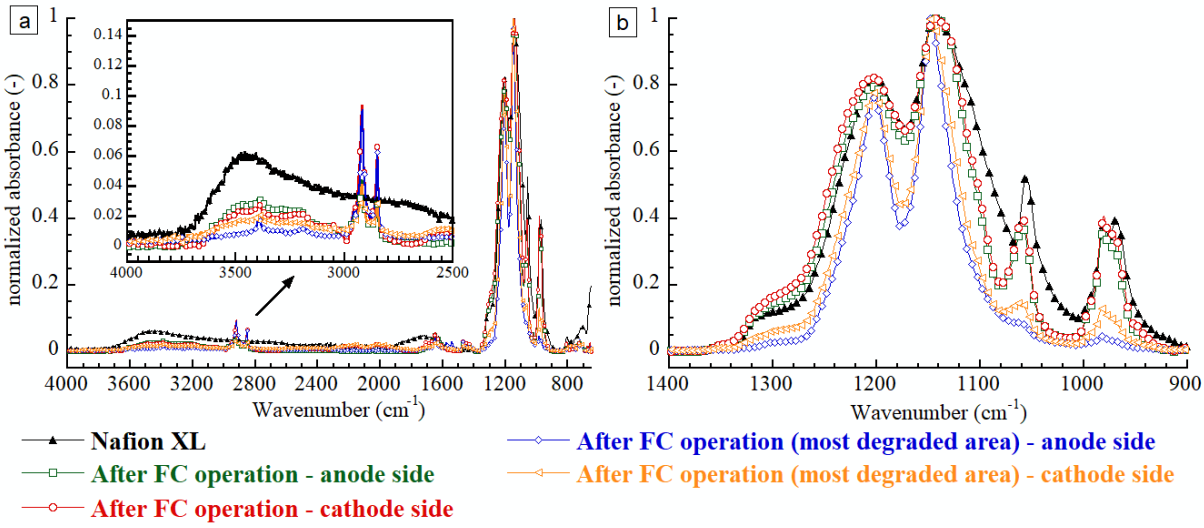


*Figure 5.* ***ATR-IR spectra of Nafion XL reinforced membrane compared to reinforced membrane after FC operation in the range (a) 4000-650 $cm^{-1}$ and (b) 1400-900 $cm^{-1}$.***

*Table 1.* ***Assignment of the IR bands of the LSC – PFSA based on literature (37-40)***

| Absorption band location ($cm^{-1}$) | Assignment |
|---|---|
| ~ 3450 | O-H stretching |
| ~ 1210 | $CF_2$ stretching, asymmetric |
| ~ 1145 | $CF_2$ stretching, symmetric |
| ~ 1055-1060 | S–O stretching, symmetric |
| ~ 980 | C–O–C (close to backbone) stretching, symmetric (39, 41, 42)<br>C–F stretching (–$CF_2$–CF($CF_3$)-group) (38, 43) |
| ~ 970 | C–O–C stretching, symmetric |